VILNIUS TECH
Vilnius Gediminas Technical University

Proceedings of the 13th International Scientific Conference

ENVIRONMENTAL ENGINEERING

April 23–24, 2026, Vilnius, LITHUANIA

eISSN 2029-7092
eISBN 978-609-476-444-8
Article ID: enviro.2026.1604
https://doi.org/10.3846/enviro.2026.1604

BIOFILM-DRIVEN H_2S BIOTRANSFORMATION IN A HIGH-SURFACE-AREA BIOFILTER PACKED WITH KOH-MODIFIED BIOCHAR AND $FECO_3$-MODIFIED CLC WASTE INOCULATED WITH *PSEUDOMONAS SPP.*

Kamyab MOHAMMADI*, Rasa VAIŠKŪNAITĖ

Department of Environmental Protection Technology and Management,
Environmental Engineering Faculty,
Vilnius Gediminas Technical University, Vilnius, Lithuania

Received 22 December 2025; revised 17 February 2026; accepted 19 February 2026

Abstract. This study provides an in-depth mechanistic assessment of H_2S biodegradation in a thermally and hydraulically controlled vertical biofilter (1.0 m height, 0.14 m width) packed with KOH-activated sewage-sludge biochar (BET 471.54 $m^2.g^{-1}$; pore volume 0.22 $cm^3.g^{-1}$) and $FeCO_3$-functionalized Cellular Lightweight Concrete (CLC) waste. *Pseudomonas* spp. were aerobically cultivated for 24 h at 30 °C to 10^7 cells.g^{-1}, then uniformly inoculated onto the media. The system was operated continuously for 144 h under 30 ± 1°C, 45–60% water-holding capacity, Empty Bed Retention Time (EBRTs) between 15–60 s, and inlet H_2S concentrations of 100–2000 ppmv, corresponding to inlet loading rates of 50–200 $g.m^{-3}h^{-1}$. Fluorescence microscopy (DAPI/SYPRO) demonstrated rapid early-stage attachment on biochar, with biomass increasing 4.1-fold within 72 h (1.4×10^6 → 5.8×10^6 cells.g^{-1}/sample). Dense, protein-rich Extracellular Polymeric Substance (EPS) matrices in stages 3–4 match the highest H_2S concentrations and maximal gas–liquid interfacial area. Hybrid biochar–CLC packing enhanced mass transfer via simultaneous physisorption, $FeCO_3$-mediated catalytic oxidation, and high-turnover enzymatic oxidation mediated by *Pseudomonas* spp. Peak removal performances were Removal Efficiency (RE) = 92–95% and Elimination Capacity (EC) = 18–22 $g.m^{-3}h^{-1}$ at 0.2–0.5 $L.min^{-1}$. Breakthrough remained negligible up to 120 h, demonstrating strong microbial–material synergy and high redox stability. $FeCO_3$-CLC promoted downstream S^0 → SO_4^{2-} conversion, stabilizing sulfur speciation under elevated loading. These findings position *Pseudomonas*–biochar systems as high-flux, kinetically resilient bio-catalytic platforms for intensified biogas desulfurization in detail.

Keywords: hydrogen sulfide biodegradation, *Pseudomonas* spp. biofiltration, KOH-activated sewage-sludge biochar, $FeCO_3$-functionalized CLC media, biogas desulfurization.

1. Introduction

Biogas production through Anaerobic Digestion (AD) of sewage sludge, agricultural residues, and mixed organic wastes has become an important renewable energy strategy worldwide (Das et al., 2022a; Franco-Morgado et al., 2018). The process offers dual benefits: converting waste streams into usable energy and reducing greenhouse gas emissions (Das et al., 2022a; Franco-Morgado et al., 2018). However, the raw biogas generated from AD systems typically contains substantial concentrations of hydrogen sulfide (H_2S), often ranging from 200 to 5,000 ppmv depending on substrate composition and digester conditions (Choudhury & Lansing, 2021). Even at relatively low concentrations, H_2S poses severe operational, environmental, and health challenges. It accelerates corrosion of pipelines, compressors, and internal combustion engines; deactivates catalysts in biogas upgrading units; reduces energy recovery efficiency; and imposes health risks to personnel. For these reasons, efficient H_2S removal is an indispensable requirement before biogas can be safely utilized for heating, electricity generation, or biomethane production (Choudhury & Lansing, 2021).

Conventional H_2S removal technologies – such as activated carbon adsorption, iron sponge systems, caustic scrubbing, and chemical oxidation – have been widely deployed in industrial applications (Zhang et al., 2021; Juntrapaporn et al., 2019; Das et al., 2022a). While effective, they come with significant drawbacks such as high chemical and replacement costs, generation of secondary waste streams, complex regeneration demands, and performance limitations under fluctuating H_2S loads typical of small- and medium-scale biogas facilities (Pudi et al., 2022; Juntrapaporn et al., 2019). These challenges have

* Corresponding author. E-mail: *kamyab.mohammadi@vilniustech.lt*

grown research interest in biological desulfurization, a process that leverages the metabolic activity of Sulfur-Oxidizing Bacteria (SOBs). Biotechnologies for H_2S removal – including bio-scrubbers, trickling filters, and biofilters – offer greener and cost-efficient alternatives by converting H_2S into environmentally benign products such as elemental sulfur (S^o) or sulfate (SO_4^{2-}) (Santos-Clotas et al., 2020; Zhang et al., 2022; Torres et al., 2020).

$$H_2S + O_2 \rightarrow S^0 + H_2O\ ; \quad (1)$$

$$S^0 + H_2O + O_2 \rightarrow SO_4^{2-} + 2H^+. \quad (2)$$

Compared with physicochemical methods, biofiltration systems require less energy, operate at ambient conditions, and utilize naturally occurring microbial communities (Bahraminia et al., 2020; Franco-Morgado et al., 2018). Nonetheless, their widespread industrial adoption is impeded by limitations in mass-transfer capacity, instability under fluctuating loading rates, long acclimation periods, and the lack of optimized packing materials capable of supporting robust microbial growth (Torres et al., 2020).

In recent years, there has been a growing scientific focus on engineered biofilter media that integrate adsorption, catalytic oxidation, and microbial colonization functionalities into a single hybrid matrix (Alkhatib et al., 2021; Das et al., 2022b). Waste-derived materials, particularly biochar and cellular concrete wastes, have attracted attention due to their low cost, environmental sustainability, favorable porosity, and customizable surface chemistry (Alkhatib et al., 2021; Das et al., 2022b). Sewage-sludge-derived biochar offers a high nutrient content, enough pore structure, and the ability to host diverse microbial communities (Santos-Clotas et al., 2020). When physically activated, its physicochemical properties can be significantly enhanced, improving both its adsorption capacity and biological compatibility (Khan et al., 2021; Ghimire et al., 2021). Likewise, Cellular Lightweight Concrete (CLC) waste, a porous material generated from the demolition and construction sectors, can be modified with iron compounds such as $FeCO_3$ to create catalytic sites that facilitate oxidation of intermediate sulfur species (Khan et al., 2021; Ghimire et al., 2021). The integration of these packing materials in a single biofiltration system aligns with circular economy principles by transforming waste into value-added adsorption–biodegradation media (Irani et al., 2018).

A further critical aspect of biofiltration is the microbial community. While traditionally dominated by Sulfur-Oxidizing Bacteria (SOB) genera such as *Acidithiobacillus* spp., recent findings have shown that *Pseudomonas* spp. – known for their metabolic versatility, rapid biofilm formation, Extracellular Polymeric Substance (EPS) secretion, and resilience to environmental fluctuations – can play a significant role in high-rate H_2S biodegradation (Jia et al., 2022; Shi et al., 2022). Their fast growth kinetics and ability to colonize complex surfaces make them strong candidates for complex biofiltration systems designed to handle high H_2S loads within compact reactor volumes (Jia et al., 2022; Shi et al., 2022).

Despite these advancements, several knowledge gaps remain. First, the mechanistic interactions between modified biochar, $FeCO_3$-impregnated CLC waste, and actively growing SOB communities are poorly understood. Specifically, it is unclear how adsorption, catalytic oxidation, and microbial oxidation compete or synergize in intense systems. Second, the spatial distribution and maturation of biofilms along the height of a vertically configured biofilter have not been comprehensively quantified, particularly under controlled thermal and hydration conditions. Third, few studies have examined the performance of hybrid biochar–CLC systems under dynamic operational regimes with varying Empty Bed Retention Times (EBRTs), loading rates, and moisture levels. Finally, the biotransformation pathways and changes in sulfur speciation ($H_2S \rightarrow S^0 \rightarrow SO_4^{2-}$) in such hybrid systems remain underexplored.

To address these gaps, this study developed a thermally stabilized, moisture-controlled, vertical biofilter packed with KOH-activated sewage-sludge biochar and $FeCO_3$-modified CLC waste, inoculated with *Pseudomonas* spp. This design integrates three synergistic mechanisms:

- Rapid physisorption of H_2S onto high-surface-area biochar, enabling immediate pollutant capture and improved mass transfer (Prasertcharoensuk et al., 2022).
- Biological oxidation mediated by *Pseudomonas* spp., facilitated by strong biofilm formation and EPS production (Prasertcharoensuk et al., 2022).
- Catalytic oxidation of intermediate sulfur species by $FeCO_3$ sites on CLC waste, promoting conversion of S^0 to SO_4^{2-} and reducing clogging risks (Prasertcharoensuk et al., 2022).

Through continuous 144 h operation, fluorescence microscopy (DAPI/SYPRO), microbial enumeration, and high-resolution gas-phase measurements, this study provides a mechanistic evaluation of biofilm-driven H_2S biotransformation in this novel hybrid biofilter. The results significantly advance understanding of material–microbe synergistic interactions and offer a foundation for designing next-generation desulfurization systems for biogas plants. Therefore, this study aims to develop and evaluate a thermally and hydraulically controlled hybrid biofilter packed with KOH-activated sewage-sludge biochar and $FeCO_3$-modified CLC waste, inoculated with *Pseudomonas* spp., for high-rate H_2S removal from biogas. The study focuses on assessing the combined roles of adsorption, microbial oxidation, and catalytic transformation under varying EBRTs and inlet H_2S loadings.

2. Methodology

2.1. Overall experimental design

The methodological framework was designed to provide a multi-scale assessment of H_2S removal in a hybrid biofilter (BF) combining adsorption, catalytic oxidation, and microbial biotransformation. This analysis took place in Vilnius Tech University's Environmental and Water Engineering laboratory. The experimental workflow consisted of 1. Preparation and modification of packing materials (biochar and CLC waste). 2. Construction of a controlled-environment BF system, including thermal, hydraulic, and flow regulation. 3. Cultivation and inoculation of *Pseudomonas* spp. onto packing media. 4. Continuous H_2S loading experiments under varied EBRTs and inlet concentrations. 5. Biofilm and microbial analyses using fluorescence microscopy (DAPI/SYPRO). 6. Evaluation of Removal Efficiency (RE), Elimination Capacity (EC), biofilm distribution, and sulfur speciation.

2.2. Biofilter construction and configuration

A custom vertical acrylic column (height = 1.0 m; internal width = 0.14 m) was designed to support transparent visibility for internal inspection, multiple sampling ports, and stable hydrodynamic behavior (Irani et al., 2018; Konkol et al., 2022; Xu et al., 2022). The reactor body was sealed with PVC flanges and silicone gaskets to prevent gas leakage. Five sampling ports (Ø 25 mm) were evenly distributed (approx. every 16 cm), enabling material extraction for microbial and chemical analysis (Figure 1). A perforated stainless-steel plate at the bottom ensured uniform gas dispersion, eliminating channeling and dead zones (Konkol et al., 2022; Xu et al., 2022).

(a) (b)

Figure 1. Vertical BF system used for microbial colonization and H_2S purification experiments, with a H_2S-containing cylinder, a rotameter, and a temperature controller: (a) – measuring the chemical composition of injected biogas into the BF – (b)

Accurate environmental control was essential to maintain microbial viability and reproducibility (Abd et al., 2022; Gao et al., 2022). For temperature regulation, a heating jacket connected to a PID controller maintained 30 ± 1 °C, optimal for *Pseudomonas* spp. growth (Abd et al., 2022; Gao et al., 2022). For moisture management, a TDR-based VH400 moisture sensor continuously monitored water-holding capacity. Moisture (45–60%) was maintained by an automated irrigation system including a peristaltic nutrient pump, mist nozzles at the top of the column, and Wi-Fi-enabled control for real-time adjustment. The BF headspace, ports, and tubing were flushed with N_2 during assembly and inoculation to minimize unintended oxygen exposure.

2.3. Packing materials selection, modification, and characterization

Raw sewage sludge was dried, ground (< 2 mm), and pyrolyzed at 500 °C under N_2 atmosphere (Cuimei et al., 2018; Watsuntorn et al., 2020). A chemical activation step with 6 M KOH was performed to increase microporosity and surface area (Cuimei et al., 2018; Watsuntorn et al., 2020). Biochar was activated at 750 °C for 1 h and rinsed to neutrality (Su & Hong, 2020). The final product exhibited a BET surface area of 471.54 $m^2.g^{-1}$, and total pore volume of 0.22 $cm^3.g^{-1}$. These properties increased H_2S adsorption capacity and improved microbial anchoring of the KOH-modified biochar derived from sewage sludge (Su & Hong, 2020; Vikrant et al., 2018). CLC waste blocks were crushed (2–5 mm), soaked in $FeCO_3$ solution, and dried at 105 °C, to increase the catalytic activity for $S^0 \rightarrow SO_4^{2-}$ oxidation (Vikrant et al., 2018). Material configurations were selected to maximize mechanistic synergy:

- Upper layers: KOH-modified biochar, to have a rapid H_2S capture;
- Middle layers: Biochar + CLC waste, to have a microbial active zone;
- Bottom layers: $FeCO_3$-impregenated CLC waste, to have a catalytic polishing and sulfur stabilization.

2.4. Microbial cultivation and inoculation

Pseudomonas spp. was selected due to rapid biofilm formation, high metabolic turnover, tolerance to fluctuating redox conditions, and the ability to colonize porous substrates (Haosagul et al., 2020; Wang et al., 2022). Cultivation was performed in nutrient broth at 30 °C for 24 h, producing ~10^7 cells.g^{-1} (Khalil et al., 2019; Haosagul et al., 2020). Packing media were sterilized at 105 °C and cooled under N_2. *Pseudomonas* spp. was sprayed uniformly onto the media and allowed to rest for 12 h for attachment (Jiao et al., 2022; Wang et al., 2022). The BF was then assembled and sealed. A 24 h acclimation period under moist, nutrient-rich conditions allowed for biofilm initiation before H_2S exposure (Jiao et al., 2022) (Figure 2).

To study microbial colonization patterns across the five BF stages, DAPI/SYPRO epifluorescence microscopy was performed (Hou et al., 2018; Moradi et al., 2020).

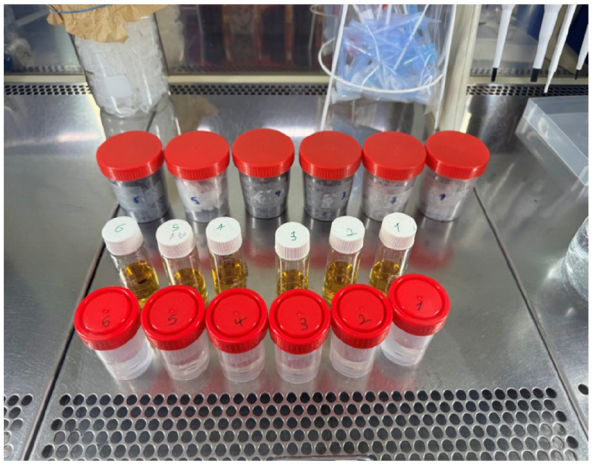

Figure 2. Stained samples of the BF's 5 stages, ready to be monitored by a microscope

Samples (~2 g) were collected from each stage and processed via 1) Fixation in 3–4% formaldehyde; 2) Triton X-100 permeabilization; 3) DAPI staining (DNA fluorescence); 4) SYPRO red staining (protein/EPS fluorescence). Samples were put in the oven for 72h (Hou et al., 2018; Moradi et al., 2020) (Figure 3).

(a) (b)

Figure 3. Packing material samples were incubated in sealed anaerobic columns – (a), and were put in an oven – (b)

Microscopy was performed using an Axioscope 5 microscope with a 100× oil-immersion objective (Khalil et al., 2019). Excitations were 340–380 nm (DAPI), 530–560 nm (SYPRO), whereas emission filters were optimized for blue/red fluorescence (Figure 4). Microbial density was estimated by counting DAPI-stained cells across 20 random fields, and normalizing counts to material mass (cells.g^{-1} equivalent) (Ma et al., 2022; Nhut et al., 2020). Image processing was done using Zen 3.2 software.

$$\mu = \frac{\ln(Nt) - \ln(N0)}{t}, \quad (3)$$

where: μ – growth rate of microbial, N_0 – initial microbial counts, N_t – counts at time, t – incubation duration (hours).

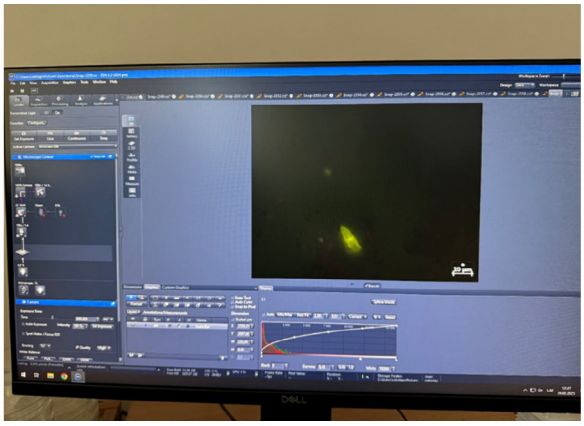

Figure 4. The Zen 3.2 software is used to visualize the surface of the samples monitored under an epifluorescence microscope

2.5. Biogas supply and operational conditions

A synthetic biogas mixture was prepared containing 100–2000 ppmv H_2S, N_2 was balanced, residual oxygen maintained below 0.3%, the flow was regulated using a mass flow controller between 0.2–1.0 L min^{-1}, and EBRTs were detected between 15, 30, 45, and 60 s (Gao et al., 2022).

The BF was operated continuously for 144 h with real-time temperature logging. Automated moisture control, hourly H_2S recordings at inlet/outlet, and daily sulfur speciation analysis (S^{2-}, S^0, SO_4^{2-}), where the regular controls were done during the experiments (Pudi et al., 2022).

H_2S concentrations at inlet and outlet ports were measured using a Gas Data Analyzer (GDA) with ±1 ppm accuracy and 2-second response time. From these measurements, RE and EC were calculated in real time (Bahraminia et al., 2020).

$$RE(\%) = \frac{Cin - Cout}{Cin} \times 100\ ; \quad (4)$$

$$EC = \frac{Q(Cin - Cout)}{V}, \quad (5)$$

where: Q – gas flow rate (m^3.h^{-1}), V – bed volume (m^3), C_{in} – inlet concentration of H_2S to BF, C_{out} – outlet concentration of H_2S from BF. The system was considered to have entered a breakthrough when RE decreased below 70%.

3. Results

3.1. Microbial colonization and biofilm evolution

Microscopic and cell-density analyses from DAPI-stained micrographs revealed a pronounced differential colonization pattern between KOH-modified biochar and $FeCO_3$-impregnated CLC waste. Biochar supported significantly denser microbial attachment, particularly within the first 72 hours, under controlled temperature

30 ± 1 °C (PID-controlled), moisture content (WHC) 45–60% (automated irrigation + sensor feedback), EBRTs 15, 30, 45, 60 s, gas flow rate 0.2–1.0 L.min^{-1}, inlet H_2S concentrations 100–2000 ppmv, inlet H_2S loading rate 50–200 g.m^{-3}h^{-1}, and oxygen concentration < 0.3% (near-anaerobic conditions). In Table 1, all operational conditions remained the same, and the impact of adding nutrient solution to the *Pseudomonas* spp. grown on biochar and CLC waste has been tested. This robust early-stage colonization can be attributed to the interconnected micropore structure and hydrophilic surface functionalities generated during the KOH activation process, which collectively enhance microbial anchoring and nutrient retention. In comparison, the $FeCO_3$-CLC waste exhibited slower but progressively structured biofilm development, which is consistent with its larger surface cavities and catalytic mineral composition that encourage more stratified, layered biofilm formation in later stages.

SYPRO Red staining revealed that EPS formation intensified substantially between 72 and 120 h, particularly within stages 3rd and 4th of the biofilter. The spatial distribution of EPS correlated strongly with the H_2S concentration distribution, suggesting that physiological stress imposed by high pollutant loading may help EPS secretion as a protective response. EPS is known to enhance microbial stability, improve immobilization of sulfur species, promote cross-cellular communication, and create microenvironments conducive to enzyme retention, all of which are essential for efficient H_2S oxidation.

The emergence of dense, protein-rich biofilms in the mid-column sections is especially noteworthy because it indicates that *Pseudomonas* spp. were not only surviving but actively adapting to the physicochemical conditions of the hybrid reactor. The thicker EPS layers in these zones act as biochemical "reactors" where dissolved sulfide and elemental sulfur (S^0) accumulate transiently and undergo further enzymatic transformations. This behavior aligns with the theoretical model of biofilters proposed by Ghimire et al. (2021), wherein the middle segments of biofilters typically exhibit the most intense biological activity due to optimized gas-to-liquid mass transfer and microbial access to substrates (Figure 5).

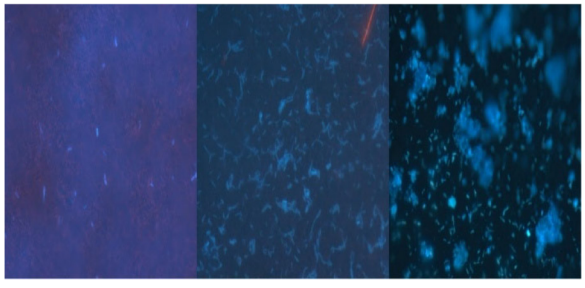

(a) (b) (c)

Figure 5. Biochar and CLC waste samples after: (a) – 24 h; (b) – after 72 h; (c) – after 120 h, inoculated with *Pseudomonas* spp., stained with DAPI and SYPRO, showing sparse individual cell attachment (100×)

Table 1. Evaluating the approximate number of existing *Pseudomonas* spp. bacteria on the biochar and CLC waste

Material	Inoculation treatment	Average count	Total bacteria / sample
Biochar	Pseudomonas	35	~1.4 × 10^6
Biochar	Nutrient + *Pseudomonas*	143	~5.8 × 10^6
CLC waste	Pseudomonas	22	~8.8 × 10^5
CLC waste	Nutrient + *Pseudomonas*	91	~3.6 × 10^6

The biofilter's internal ecosystem evolved into a distinct stratified structure, with each stage contributing differently to the sequential stages of H_2S transformation.

In stages 1–2, sorption processes dominated. Limited EPS development, along with high DAPI counts but low SYPRO fluorescence, and a sharp H_2S decrease (> 30% drop within the top 20 cm) was detected. The abundance of micropores and the large surface area of biochar enabled rapid H_2S capture, reducing gas-phase concentrations before they reached deeper layers. This initial removal eases the burden on downstream microbial communities, effectively "pre-conditioning" the gas stream to levels more favorable for enzymatic oxidation.

In stages 3rd and 4th, a major shift occurred from sorption-dominated to bio-oxidation-dominated behavior. Peak cell density (over 6.1×10^6 cells.g^{-1}/sample), abundant EPS (highest SYPRO intensities), and strong S^0 accumulation (microscopically visible as yellowish particulates) were detected. Maximum H_2S removal rates (up to 22 g.m^{-3}.h^{-1}). These zones exhibited the highest microbial densities, the richest EPS matrices, and the largest pools of intermediate sulfur species. The pronounced accumulation of S^0 observed here suggests that microbial oxidation of H_2S was proceeding vigorously but had not yet fully transitioned to sulfate production. These zones, therefore, represent the biochemical core where biological sulfur cycling is most active (Figure 6 and Figure 7).

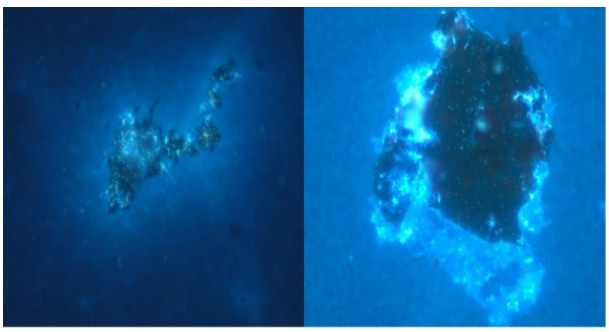

(a) (b)

Figure 6. DAPI and SYPRO-stained image of biochar from: (a) – stage 3; (b) – stage 4 with *Pseudomonas* spp. showing attached bacteria and created a colony

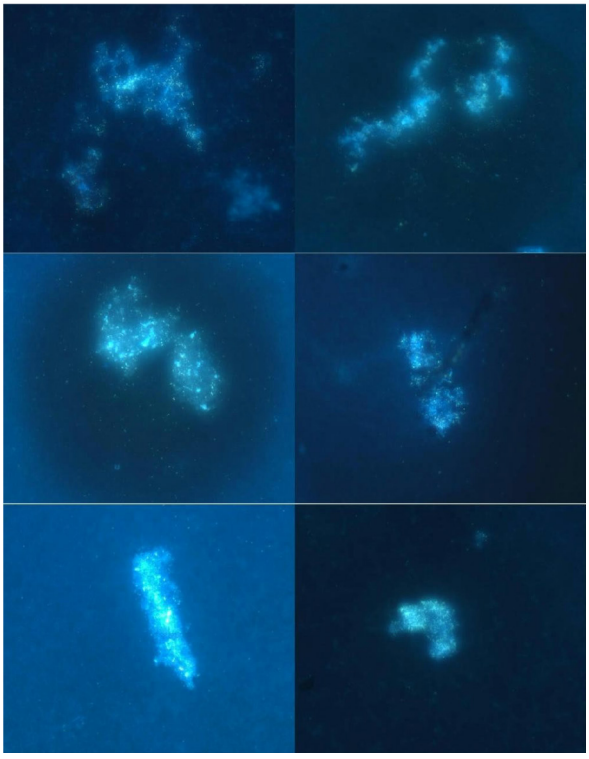

Figure 7. DAPI and SYPRO-stained image of CLC waste from stage 1–6 with *Pseudomonas* spp. showing dense colonization

In stages 5–6, catalytic oxidation processes gained prominence. Higher sulfate (SO_4^{2-}) accumulation, moderate microbial density, but high catalytic activity, and stabilization of sulfur species were detected. Prevention of clogging by sulfur deposits. Although microbial densities were lower than in the upper and middle layers, $FeCO_3$ presence promoted downstream oxidation of S^0 into SO_4^{2-}, minimizing potential clogging issues and enabling the system to maintain long-term operational stability. This catalytic polishing stage is critical because many biofilters fail due to sulfur accumulation; here, the hybrid media prevented this failure pathway by stabilizing sulfur speciation.

3.2. Biofilter start-up dynamics and early-stage stabilization

The hybrid biofilter exhibited a rapid and stable start-up, demonstrating that the engineered packing materials and inoculated *Pseudomonas* spp. collectively facilitated the establishment of a biocatalytic environment. Initial inlet concentrations ranged between 100 and 600 ppmv H_2S, depending on selected loading conditions. During the initial 24 h period, the outlet H_2S concentration decreased progressively despite the biofilm being at an early developmental stage, indicating that the physical and chemical attributes of the KOH-activated biochar and $FeCO_3$-impregnated CLC waste played a dominant role in the initial sorption-driven removal of H_2S. Within the first 72 h, while the number of bacteria is significant 4.20E+07, and in the second stages 7.30E+07 showed a slight increase, the number of the *Pseudomonas* spp. significant and notably high. The highest numbers were detected on the 3rd (1.15E+08) and 4th (1.15E+08) stages of the biofilter, which also reported a high level of H_2S removal efficiency. The last stage (fifth) showed a decrease in the number of *Pseudomonas* spp., which matches the decline in RE of H2S from biogas detected by GDA. Notably, this behavior contrasts with traditional biofilters, where the start-up phase is often prolonged due to reliance on strict biological processes; here, physicochemical sorption bridged the lag period typically associated with microbial adaptation, allowing a smoother transition into full biological activity (Table 2).

3.3. H_2S removal performance and influence of EBRT

The hybrid biofilter consistently achieved high removal efficiencies (92–95%) after the initial stabilization period. Even with relatively short EBRTs of 15–30 s, the system-maintained removal efficiencies above 80% from 48 h to 120 h, highlighting its ability to operate under high-throughput conditions while maintaining system-maintained performance trade-offs. Negligible breakthroughs occurred during the first 120 h, even at high loadings. This is especially important for real-world biogas upgrading applications where flow fluctuations and limited retention times are common (Figure 8). The results are comparable to or higher than those reported for conventional biofilters and bio-trickling filters treating H_2S. For instance, Vikrant et al. (2018) reported RE values of 80–90% for compost- and volcanic-rock-based biofilters operating at EBRTs above 60 s, while Juntrapaporn et al. (2019) observed stable RE of approximately 85–90% in bio-trickling filters inoculated with *Paracoccus pantotrophus*. The higher RE obtained in the present system, even at EBRTs as short as 15–30 s, indicates that the hybrid biochar–CLC packing enhances mass transfer and biological activity under intensified operating conditions.

EC followed a characteristic growth curve: a) start-up (0–24 h) between 5–8 $g.m^{-3}h^{-1}$, mid-phase (24–72 h) between 12–18 $g.m^{-3}h^{-1}$, and peak performance (72–120 h) between 18–22 $g.m^{-3}h^{-1}$. As mentioned, initial low values indicative of sorption-only behavior gradually transitioned to higher EC values, as microbial oxidation became dominant. The maximum elimination capacity reached 18–22 g H_2S m^{-3} h^{-1}, which exceeds values commonly reported for single-media biofilters. Typical EC values reported for compost-based biofilters range from 5 to 15 $g.m^{-3}h^{-1}$ (Bahraminia et al., 2020; Vikrant et al., 2018), while biotrickling filters using inert packing materials often achieve ECs of 10–20 $g.m^{-3}h^{-1}$ but require higher liquid recirculation and more complex operation (Juntrapaporn et al., 2019; Torres et al., 2020). The elevated EC observed here can be attributed to the synergistic combination of high-surface-area biochar for rapid

H_2S capture, robust Pseudomonas biofilms, and $FeCO_3$-mediated catalytic oxidation of sulfur intermediates.

EBRT significantly influenced system stability. Longer EBRTs (45–60 s) resulted in maximum RE (94–95%), lowest outlet H_2S concentrations, the thickest and most uniform biofilms, and highest EPS formation. It allowed greater contact time for complete oxidation, whereas moderate EBRTs (30 s or 15 s) resulted in slightly reduced RE (89% or 80%), high EC maintained, and balanced sorption–biodegradation performance. Achieving high H_2S removal at short EBRTs is a critical requirement for compact biogas upgrading systems. Previous studies have shown that EBRTs above 45–60 s are often necessary to maintain stable performance in conventional biofilters (Santos-Clotas et al., 2020; Nhut et al., 2020). In contrast, the present biofilter maintained removal efficiencies above 80% at EBRTs as low as 15 s, highlighting its suitability for high-throughput applications. This performance is consistent with recent efforts to intensify biofiltration through engineered media and targeted microbial inoculation (Das et al., 2022b).

Comprehensive sulfur speciation analysis revealed that H_2S undergoes a series of transformations along the reactor height. Dissolved sulfide concentrations were highest in Stage 1, reflecting initial dissolution, while S^0 concentrations peaked in the biologically active mid-sections, confirming that microbial activity favored partial oxidation. Finally, the highest sulfate concentrations were detected in the bottom zones where $FeCO_3$ catalyzed further oxidation. This sequential transformation pattern from H_2S to S^0 and then SO_4^{2-} provides strong evidence that the biofilter operates as a multi-stage hybrid reactor, where each layer contributes uniquely to the overall removal mechanism. The presence of $FeCO_3$ significantly boosted the conversion of sulfur intermediates into more stable forms, ensuring that sulfur cycling did not lead to biomass inhibition or pore clogging, which are common failure modes in single-material biofilters.

Table 2. Comparative summary of microbial density and H_2S removal for *Pseudomonas* spp. across different BF stages

Biofilter stages	H_2S removal (%)	Microbial density (cells/g)
1	45	4.20E+07
2	58	7.30E+07
3	78	1.15E+08
4	81	1.05E+08
5	63	9.10E+07

Breakthrough analysis demonstrated remarkable system robustness. No significant breakthrough (RE < 70%) was observed until beyond 120 h. Even during the final 24 h period, outlet concentrations increased only marginally, indicating that both sorption sites and microbial activity remained effective over the test duration. The pressure drop across the reactor remained stable as well, confirming that the design effectively mitigated sulfur accumulation – a key advantage of integrating catalytic and biological processes.

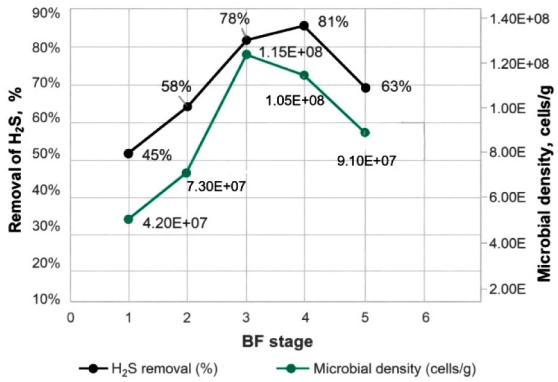

Figure 8. Correlation of H_2S removal and microbial density by BF stages

4. Conclusions

This study demonstrates that integrating KOH-activated sewage-sludge biochar with $FeCO_3$-functionalized CLC waste, inoculated with *Pseudomonas* spp., creates a highly efficient system for H_2S bio-desulfurization. The hybrid biofilter achieved 92–95% removal efficiency and elimination capacities up to 22 ± 1.4 $g.m^{-3}h^{-1}$, with stable performance observed across variable EBRTs.

These analyses revealed that microbial colonization was both statistically significant and spatially structured. Biochar-supported upper zones showed rapid early attachment ($1.4\times10^6 \rightarrow 5.8\times10^6$ $cells.g^{-1}$ within 72 h), confirming the role of high surface area in accelerating start-up. Mid-column zones (stages 3–4) exhibited the highest biomass and the strongest EPS signals (2–3× greater than stages 1–2), corresponding to the highest H_2S oxidation rates and serving as the biochemical core of the system.

The integration of controlled operational and microbial growth conditions resulted in low pressure drop ($\Delta P < 15$ $Pa{\cdot}m^{-1}$), delayed breakthrough (> 120 h), and robust performance under short EBRTs – features essential for compact biogas purification systems. The success of waste-derived media also demonstrates a pathway toward economically and environmentally sustainable biofiltration designs.

Future work should expand into long-term continuous testing, optimization of biochar–CLC ratios, and mixed inoculation to further enhance sulfur cycling and broaden operational robustness. Nonetheless, this study provides strong evidence – supported by microbial quantification, EPS profiling, and statistical validation – that hybrid biofilters can achieve superior H_2S removal through synergistic material–microbe interactions and spatially organized biofilm activity.

References

Abd, A. A., & Othman, M. R. (2022). Biogas upgrading to fuel grade methane using pressure swing adsorption: Parametric sensitivity analysis on an industrial scale. *Fuel*, *308*, Article 121986. https://doi.org/10.1016/j.fuel.2021.121986

Alkhatib, I. I. I., Khalifa, O., Bahamon, D., Abu-Zahra, M. R. M., & Vega, L. F. (2021). Sustainability criteria as a game changer in the search for hybrid solvents for CO2 and H_2S removal. *Separation and Purification Technology*, *277*, Article 119516. https://doi.org/10.1016/j.seppur.2021.119516

Bahraminia, S., Anbia, M., & Koohsaryan, E. (2020). Hydrogen sulfide removal from biogas using ion-exchanged nanostructured NaA zeolite for fueling solid oxide fuel cells. *International Journal of Hydrogen Energy*, *45*(55), 31027–31040 https://doi.org/10.1016/j.ijhydene.2020.08.091

Choudhury, A., & Lansing S. (2021). Adsorption of hydrogen sulfide in biogas using a novel iron-impregnated biochar scrubbing system. *Journal of Environmental Chemical Engineering*, *9*(1), Article 104837. https://doi.org/10.1016/j.jece.2020.104837

Cuimei, B., Wei, G., Chao, T., Jun, L., & Xiaohua, L. (2018). Dynamic control design and simulation of biogas pressurized water scrubbing process. *IFAC-PapersOnline*, *51*(18), 560–565. https://doi.org/10.1016/j.ifacol.2018.09.365

Das, J., Ravishankar, H., & Lens, P. N. L. (2022a). Biological biogas purification: Recent developments, challenges and future prospects. *Journal of Environmental Management*, *304*, Article 114198. https://doi.org/10.1016/j.jenvman.2021.114198

Das, J., Nolan, S., & Lens, P. N. L. (2022b). Simultaneous removal of H_2S and NH_3 from raw biogas in hollow fiber membrane bioreactors. *Environmental Technology & Innovation*, *28*, Article 102777. https://doi.org/10.1016/j.eti.2022.102777

Franco-Morgado, M., Toledo-Cervantes, A., González-Sánchez, A., Lebrero, R., & Muñoz, R. (2018). Integral (VOCs, CO_2, mercaptans and H_2S) photosynthetic biogas upgrading using innovative biogas and digestate supply strategies. *Chemical Engineering Journal*, *254*, 363–369. https://doi.org/10.1016/j.cej.2018.08.026

Gao, Y., Han, Z., Zhai, G., Dong, J., & Pa, X. (2022). Oxidation absorption of gaseous H_2S using UV/$S_2O_8^{2-}$ advanced oxidation process: Performance and mechanism. *Environmental Technology & Innovation*, *25*, Article 102124. https://doi.org/10.1016/j.eti.2021.102124

Ghimire, A., Gyawali, R., Lens, P. N. L., & Lohani S. P. (2021). Chapter 110 – Technologies for removal of hydrogen sulfide (H_2S) from biogas. In *Emerging technologies and biological systems for biogas upgrading* (pp. 295–230). Academic Press. https://doi.org/10.1016/B978-0-12-822808-1.00011-8

Haosagul, S., Prommeenate, P., Hobbs, G., & Pisutpaisal, N. (2020). Sulfur-oxidizing bacteria in full-scale biogas cleanup system of ethanol industry. *Renewable Energy*, *150*, 965–972. https://doi.org/10.1016/j.renene.2019.11.140

Hou, N., Xia, Y., Wang, X., Liu, H., Liu, H., & Xun L. (2018). H_2S biotreatment with sulfide-oxidizing heterotrophic bacteria. *Biodegradation*, *29*, 511–524. https://doi.org/10.1007/s10532-018-9849-6

Irani, V., Tavasoli, A., & Vahidi, M. (2018). Preparation of amine functionalized reduced graphene oxide/methyl diethanolamine nanofluid and its application for improving the CO_2 and H_2S absorption. *Journal of Colloid and Interface Science*, *527*, 57–67. https://doi.org/10.1016/j.jcis.2018.05.018

Jia, T., Sun, S., Zhao, Q., Peng, Y., & Zhang, L. (2022). Extremely acidic condition (pH < 1.0) as a novel strategy to achieve high-efficient hydrogen sulfide removal in biotrickling filter: Biomass accumulation, sulfur oxidation pathway and microbial analysis. *Chemosphere*, *294*, Article 133770. https://doi.org/10.1016/j.chemosphere.2022.133770

Jiao, Y., Han, S., Zhang, W., Guo, M., Cheng, F., & Zhang, M. (2022). Self-assembled CuO-bearing aerogel-like hollow Al_2O_3 microspheres for room temperature dry capture of H_2S. *Chemical Engineering Research and Design*, *177*, 174–183. https://doi.org/10.1016/j.cherd.2021.10.030

Juntrapaporn, J., Vikromvarasiri, N., Soralump, C., & Pisutpaisal, N. (2019). Hydrogen sulfide removal from biogas in biotrickling filter system inoculated with *Paracoccus pantotrophus*. *International Journal of Hydrogen Energy*, *44*(56), 29554–29560. https://doi.org/10.1016/j.ijhydene.2019.03.069

Khan, M. U., En Lee, J. T., Bashir, M. A., Dissanayake, P. D., Ok, Y. S., Tong, Y. W., Shariati, M. A., Wu, S., & Ahring, B. K. (2021). Current status of biogas upgrading for direct biomethane use: A review. *Renewable and Sustainable Energy Reviews*, *149*, Article 111343. https://doi.org/10.1016/j.rser.2021.111343

Khalil, M., Berawi, M. A., Heryanto, R., & Rizalie, A. (2019). Waste to energy technology: The potential of sustainable biogas production from animal waste in Indonesia. *Renewable and Sustainable Energy Reviews*, *105*, 323–331. https://doi.org/10.1016/j.rser.2019.02.011

Konkol, D., Popiela, E., Skrzypczak, D., Izydorczyk, G., Mikula, K., Moustakas, K., Opaliński, S., Korczyński, M., Witek-Krowiak, A., & Chojnacka, K. (2022). Recent innovations in various methods of harmful gases conversion and its mechanism in poultry farms. *Environmental Research*, *214*, Article 113825. https://doi.org/10.1016/j.envres.2022.113825

Kulawong, S., Artkla, R., Sriprapakhan, P., & Maneechot, P. (2022). Biogas purification by adsorption of hydrogen sulfide on NaX and Ag-exchanged NaX zeolites. *Biomass and Bioenergy*, *159*, Article 106417. https://doi.org/10.1016/j.biombioe.2022.106417

Ma, C., Zhao, Y., Chen, H., Liu, Y., Huang, R., & Pan, J. (2022). Biochars derived from by-products of microalgae pyrolysis for sorption of gaseous H_2S. *Journal of Environmental Chemical Engineering*, *10*(3), Article 107370. https://doi.org/10.1016/j.jece.2022.107370

Moradi, H., Azizpour, H., Bahmanyar, H., & Mohammadi, M. (2020). Molecular dynamics simulation of H_2S adsorption behavior on the surface of activated carbon. *Inorganic Chemistry Communications*, *118*, Article 108048. https://doi.org/10.1016/j.inoche.2020.108048

Nhut, H. H., Thanh, V. L. T., & Le, L. T. (2020). Removal of H_2S in biogas using biotrickling filter: Recent development. *Process Safety and Environmental Protection*, *144*, 297–309. https://doi.org/10.1016/j.psep.2020.07.011

Pudi, A., Rezaei Sarkhanlou, M., Signorini V., Andersson M. P., Baschetti, M. G., & Mansouri, S. S. (2022). Hydrogen sulfide capture and removal technologies: A comprehensive review of recent developments and emerging trends. *Separation and Purification Technology*, *298*, Article 121448. https://doi.org/10.1016/j.seppur.2022.121448

Prasertcharoensuk, P., Promtongkaew, A., Tawatchai, M., Marquez, V., Jongsomjit, B., Tahir, M., Praserthdam, S., & Praserthdam, P. (2022). A review on sensitivity of operating parameters on biogas catalysts for selective oxidation of Hydrogen Sulfide to elemental sulfur. *Chemosphere*, *301*, Article 134579. https://doi.org/10.1016/j.chemosphere.2022.134579

Santos-Clotas, E., Cabrera-Codony, Comas J., & Martín, M. J. (2020). Biogas purification through membrane bioreactors: Experimental study on siloxane separation and biodegradation. *Separation and Purification Technology*, *238*, Article 116440. https://doi.org/10.1016/j.seppur.2019.116440

Shi, M., Xiong, W., Zhang, X., Ji, J., Hu, X., Tu, Z., Wu, Y. (2022). Highly efficient and selective H_2S capture by task-specific deep eutectic solvents through chemical dual-site absorption. *Separation and Purification Technology*, *283*, Article 120167. https://doi.org/10.1016/j.seppur.2021.120167

Su, J.-J., & Hong, Y.-Y. (2020). Removal of hydrogen sulfide using a photocatalytic livestock biogas desulfurizer. *Renewable Energy*, *149*, 181–188. https://doi.org/10.1016/j.renene.2019.12.068

Torres, R. A., Marín, D., Rodero, M. D. R., Pascual, C., González-Sanchez, A., de Godos Crespo, I., Lebrero, R., & Torre, R. M. (2020). Chapter 8 – Biogas treatment for H_2S, CO_2, and other contaminants removal. In *From biofiltration to promising options in gaseous fluxes biotreatment* (pp. 153–176). Elsevier. https://doi.org/10.1016/B978-0-12-819064-7.00008-X

Vikrant, K., Kailasa, S. K., Tsang, D. C. W., Lee, S. S., Kumar, P., Giri, B. S., Singh, R. S., Kim, K.-H. (2018). Biofiltration of hydrogen sulfide: Trends and challenges. *Journal of Cleaner Production*, *187*, 131–147. https://doi.org/10.1016/j.jclepro.2018.03.188

Wang, S., Nam, H., Lee, D., & Nam, H. (2022). H_2S gas adsorption study using copper impregnated on KOH activated carbon from coffee residue for indoor air purification. *Journal of Environmental Chemical Engineering*, *10*(6), Article 108797. https://doi.org/10.1016/j.jece.2022.108797

Watsuntorn, W., Khanongnuch, R., Chulalaksananuku, W., Rene, E. R., Lens P. N. L. (2020). Resilient performance of an anoxic biotrickling filter for hydrogen sulfide removal from a biogas mimic: Steady, transient state and neural network evaluation. *Journal of Cleaner Production*, *249*, Article 119351. https://doi.org/10.1016/j.jclepro.2019.119351

Xu, Y., Chen, Y., Ma, C., Qiao, W., Wang, J., & Ling, L. (2022). Functionalization of activated carbon fiber mat with bimetallic active sites for NH_3 and H_2S adsorption at room temperature. *Separation and Purification Technology*, *303*, Article 122335. https://doi.org/10.1016/j.seppur.2022.122335

Zhang, X., Lawan, I., Danhassan, U. A., He, Y., Qi, R., Wu, A., Sheng, K., & Lin H. (2022). Chapter three – Advances in technologies for in situ desulfurization of biogas. *Advances in Bioenergy*, *7*, 99–137. https://doi.org/10.1016/bs.aibe.2022.05.001

Zhang, Y., Kawasaki, Y., Oshita, K., Takaoka, M., Minami, D., Inoue, G., & Tanaka T. (2021). Economic assessment of biogas purification systems for removal of both H_2S and siloxane from biogas. *Renewable Energy*, *168*, 119–130. https://doi.org/10.1016/j.renene.2020.12.058